

# Preclinical investigations of anti-glypican-1 antibody-drug conjugate as an anticancer agent for glypican-1–positive uterine cervical cancer

Satoko Matsuzaki<sup>1,3</sup>, Satoshi Serada<sup>2,3</sup>, Kosuke Hiramatsu<sup>2,3</sup>, Satoshi Nojima<sup>4</sup>, Shinya Matsuzaki<sup>1</sup>, Yutaka Ueda<sup>1</sup>, Kiyoshi Yoshino<sup>1</sup>, Seiji Mabuchi<sup>1</sup>, Minoru Fujimoto<sup>2,3</sup>, Eiichi Morii<sup>4</sup>, Tadashi Kimura<sup>1</sup>, Tetsuji Naka<sup>2,3</sup>

<sup>1</sup>Department of Obstetrics and Gynecology, Osaka University Graduate School of Medicine, <sup>2</sup>Center for Intractable Immune Disease, Kochi Medical School, Kochi University, <sup>3</sup>Laboratory of Immune Signal, National Institutes of Biomedical Innovation, Health and Nutrition, <sup>4</sup>Department of Pathology, Osaka University Graduate School of Medicine

## ABSTRACT

Glypican-1 (GPC1) is highly expressed in solid tumors, especially squamous cell carcinomas (SCCs). We explored the use of a GPC1-targeted antibody-drug conjugate (ADC) as a novel treatment for uterine cervical cancer. Our data showed that GPC1-ADC has potential as a novel therapy for uterine cervical cancer. In particular, it may be useful for both new-onset cancer and for tumors that relapse after concurrent chemoradiotherapy.

## INTRODUCTION

Antibody-drug conjugates (ADC) were developed to improve the therapeutic indices of cytotoxic anticancer agents. This approach uses an immunocjugate in which a cytotoxic agent is chemically or enzymatically linked to an antibody that selectively binds to an internalizing tumor-associated antigen. This strategy allows specific delivery of the cytotoxic agent to the tumor site while minimizing the exposure of normal tissues to the drug. Although ADCs have been shown to be potent targeted treatment for various cancers, no previous study of an ADC for cervical cancer has been reported. Recently, our group identified glypican-1 (GPC1) as a novel cancer antigen in esophageal squamous cell carcinoma (ESCC) by a quantitative proteomic approach focused on cell surface membrane proteins. We confirmed the limited or relatively low expression of GPC1 in normal tissues compared with ESCC tissues. We also demonstrated that targeting GPC1 with an anti-GPC1 monoclonal antibody (mAb) had a strong antitumor effect *via* antibody-dependent cellular cytotoxicity and complement-dependent cytotoxicity in both a dependent and independent manner. Importantly, anti-GPC1 mAb also induced potent tumor growth inhibition in xenograft models using patient-derived GPC1-positive ESCC tumors, suggesting that GPC1 would be a promising therapeutic target in ESCC. This study aimed to assess the expression of GPC1 in uterine cervical cancer and investigate the possibility of it being a new therapeutic target, with GPC1-ADC as a novel drug delivery technology.

## MATERIALS AND METHODS

Immunostaining was scored according to the intensity of the staining: 0, no staining; 1, weak staining (i.e., lower than in the basal layer); 2, strong staining (the same or stronger as in the basal layer). The density of staining was as follows: 0, indicated 0%–9% positivity; 1, indicated 10%–40%; 2, indicated 41%–70%; and 3, indicated 71%–100% positivity. The final immunohistochemistry (IHC) score was determined by multiplying the intensity score by the density score, resulting in a maximum possible score of 6. Patient characteristics are shown in Table 1.

**TABLE 1** Characteristics of tumors from patients with cancer of the uterine cervix

	SCC	AC
Number of cases	68	42
Age, (years) median (range),	45.5 (26–74)	46.5 (24–66)
FIGO stage		
IA2	1	0
IB1	41	30
IB2	9	6
IIA	3	4
IIB	14	2
Tumor size		
≤4 cm	31	28
>4 cm	37	14

AC, adenocarcinoma; FIGO, International Federation of Gynaecology and Obstetrics; SCC, squamous cell carcinoma

- Two human cervical cancer cell lines (HeLa [AC] and ME180 [SCC]) and a human ovarian clear cell carcinoma cell line (RMG-1) were obtained from the Japanese Collection of Research Bioresources (Osaka, Japan).
- Cell surface GPC1 expression levels were quantified with QIAGEN flow cytometric indirect immunofluorescence assay (Dako, Hamburg, Germany) using anti-GPC1 mAb (clone 01a033) as the primary antibody.
- The anti-GPC1 mAb (clone 01a033) and isotype control antibody (mouse IgG2a, clone MOPC-173, BioLegend, San Diego, CA) were used to manufacture the ADC.
- The drug-to-antibody ratio as determined by the ratio of A248nm:A280nm was 4.1 for GPC1-ADC and 3.8 for the control-ADC.
- The drug distribution was analyzed by hydrophobic interaction chromatography.

## RESULTS

Among SCCs, 38 cases (55.9%) scored more than 4 points (“Strong” group), 24 cases (35.3%) scored 1 to 3 points (“Low” group), and 6 cases (9%) scored 0 points (“Negative” group). Among ACs, 21 cases (50%) were in the Strong group, 14 (33.3%) in the Low group, and 7 (16.7%) in the Negative group. Interestingly, expression of GPC1 was also detected in tissue from a relapsed SCC of the uterine cervix after chemoradiation therapy (Figure 1).

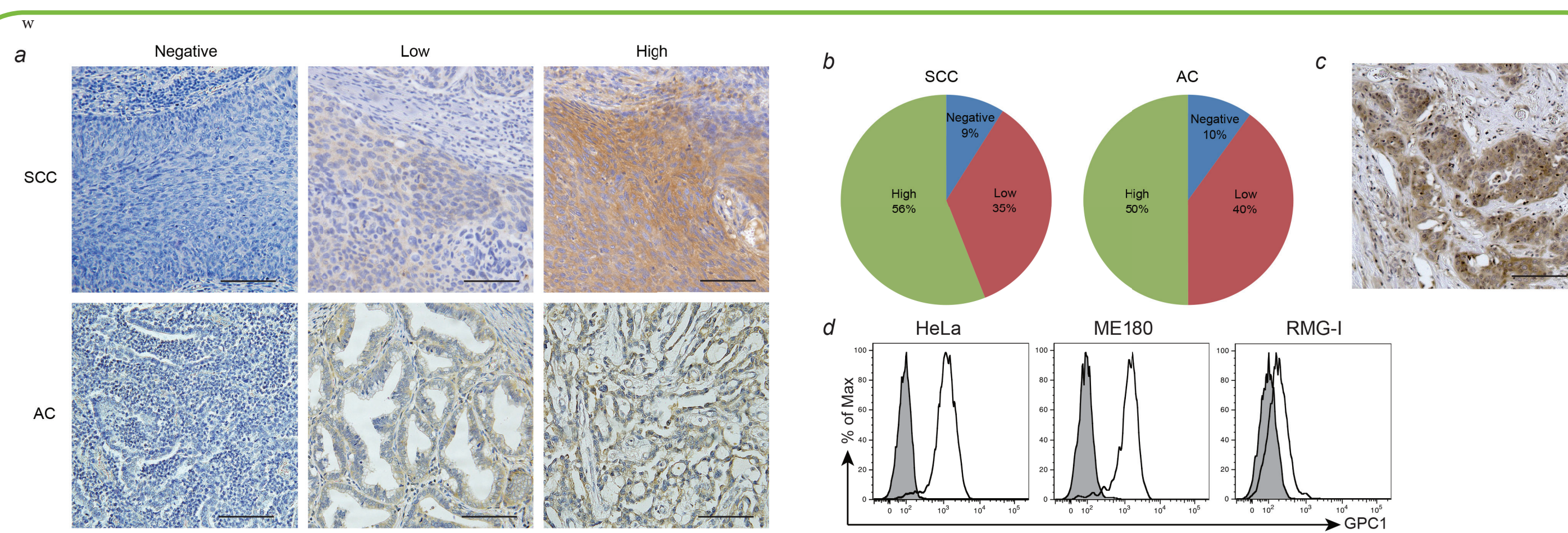


**Figure 1** Immunohistochemical analysis of GPC1 expression in clinical cervical cancer specimens.

*a*, Representative images of various intensities of IHC staining for GPC1 in tissue specimens of cervical SCC and AC. *b*, The graphs represent the percentages of GPC1 expression scores in tumor samples from patients with cervical SCC and AC. Most are GPC1-positive. *c*, Representative images of IHC staining for GPC1 in tissue from a relapsed cervical SCC after chemoradiation therapy. *d*, Flow cytometry of GPC1 expression in HeLa, ME180, and RMG-1 cells detected with an anti-GPC1 monoclonal antibody.

HeLa and ME180 cell lines had high expression levels of GPC1, while the expression of GPC1 was low in RMG-1 cells. GPC1 was highly expressed in the cervical cancer cell lines in addition to the clinical specimens. The GPC1-binding activities of the mAbs were confirmed by flow cytometry using a GPC1-positive cell line and surface plasmon resonance analysis. mAbs were screened based on their ability to deliver an auristatin payload into GPC1-expressing cells *in vitro* using a high-throughput indirect cytotoxicity assay exposing cells to anti-GPC1 mAb and MMAF-conjugated secondary antibody. Among 18 mAbs, clone 01a033 most efficiently delivered the MMAF-conjugated secondary antibody into GPC1-positive cells (Table 2). We therefore selected clone 01a033 for the antibody component of the GPC1-ADC, and anti-GPC1 mAb 01a033 or an isotype control mouse IgG2a were directly conjugated with MMAF (Figure 2*a*). The internalization of GPC1-ADC occurred rapidly in both cell lines (Figure 2*c*). To confirm the translocation of GPC1-ADC to lysosomes, immunofluorescence analysis was performed, which had already been used to show GPC1-ADC binding to the cell membranes when preincubated at 4°C before the internalization assay. When GPC1-ADC exposed cells were incubated at 37°C for 4h (Figure 2*d*), GPC1-ADC membrane staining was decreased and GPC1-ADC was found instead in the lysosomes, as evidenced by the overlap of staining for GPC1-ADC and the lysosomal marker LAMP-1 (Figure 2*d*). These results suggest that GPC1-ADC is first bound to the membrane of GPC1-expressing cells and is then internalized and translocated to the lysosomal compartment.

**TABLE 2** IC<sub>50</sub> values for MMAF, GPC1-ADC, and control-ADC in uterine cervix and ovarian cancer cell lines

Cell lines	Morphology	GPC1 expression (ABC/cell)	GPC1-ADC (nM)	Control-ADC (nM)	MMAF (nM)
HeLa	Epithelioid carcinoma	53,884	0.042	N.D.	29.7
ME180	Squamous cell carcinoma	78,437	0.093	N.D.	35.4
RMG-1	Ovarian clear cell carcinoma	5,817	N.D.	N.D.	136.3

ABC, antibody-binding capacity; ADC, antibody-drug conjugate; GPC1, glypican-1; MMAF, monomethyl auristatin; N.D., none detected

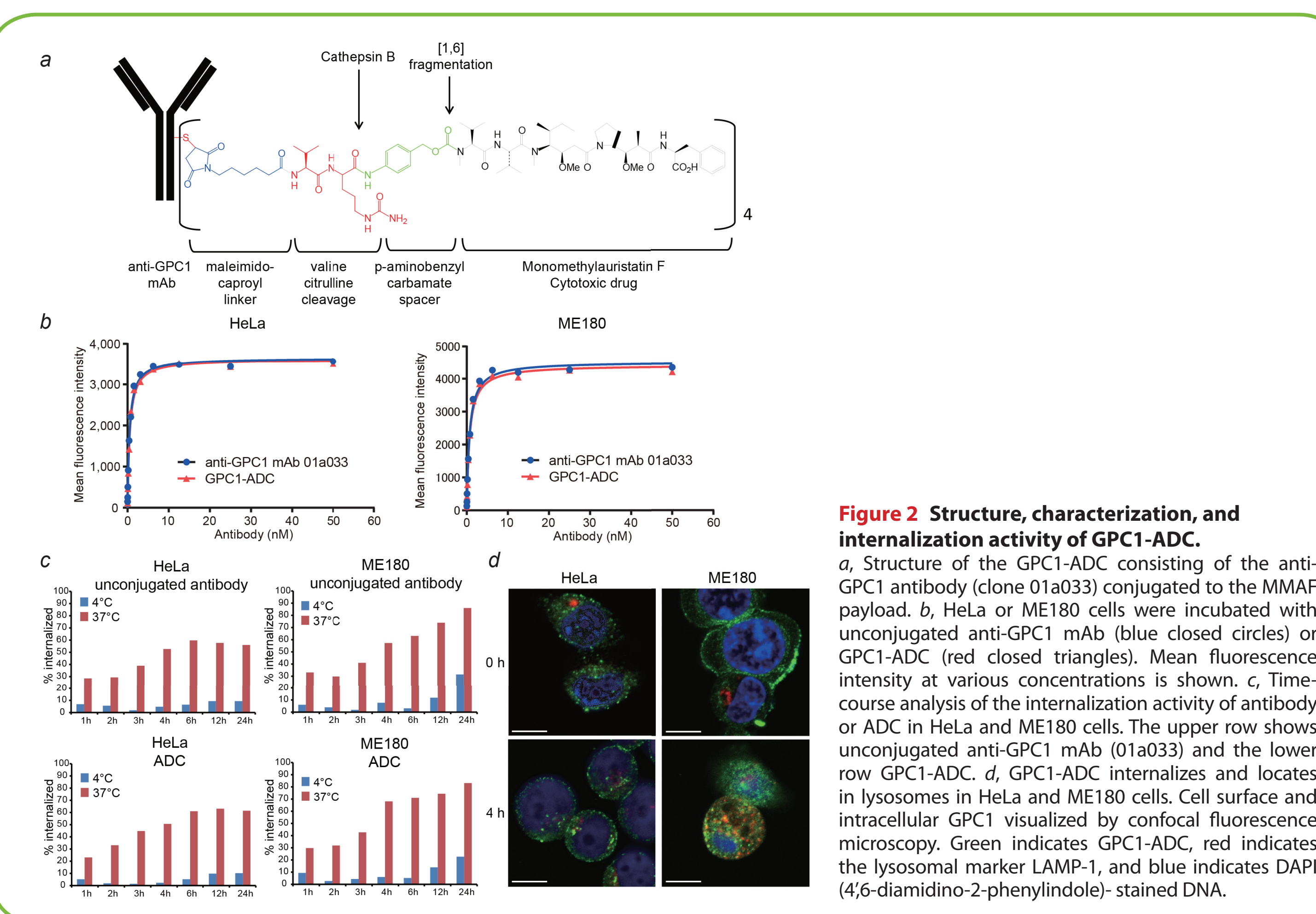


**Figure 2** Structure, characterization, and internalization activity of GPC1-ADC.

*a*, Structure of the GPC1-ADC consisting of the anti-GPC1 antibody (clone 01a033) conjugated to the MMAF payload. *b*, HeLa or ME180 cells were incubated with unconjugated anti-GPC1 mAb (blue closed circles) or GPC1-ADC (red closed triangles). Mean fluorescence intensity at various concentrations is shown. *c*, Time-course analysis of the internalization activity of antibody or ADC in HeLa and ME180 cells. The upper row shows unconjugated anti-GPC1 mAb (01a033) and the lower row GPC1-ADC. *d*, GPC1-ADC internalizes and locates in lysosomes in HeLa and ME180 cells. Cell surface and intracellular GPC1 visualized by confocal fluorescence microscopy. Green indicates GPC1-ADC, red indicates the lysosomal marker LAMP-1, and blue indicates DAPI (4',6-diamidino-2-phenylindole)-stained DNA.

While unconjugated anti-GPC1 mAb had no effect on the viability of any of the cell lines, GPC1-ADC caused a dose-dependent decrease in cell viability in both HeLa and ME180 cells *in vitro* (Figures 3*a* and *b*). The IC<sub>50</sub> value of GPC1-ADC was 0.042 nM for HeLa and 0.093 nM for ME180 cells (Table 2). Unconjugated anti-GPC1 mAb showed no cytotoxicity at concentrations up to 666.6 μM. Since MMAF impairs cell membrane permeability, the sensitivity of cells to unconjugated MMAF was not high, as shown by IC<sub>50</sub> values of MMAF between 29.7 to 136.3 nM against each of the cell lines (Table 2). GPC1-ADC is internalized into the lysosome, presumably then releasing the MMAF to exert its toxic effects. The cytotoxicity of the GPC1-ADC against GPC1-positive cells was also shown to be concentration dependent.

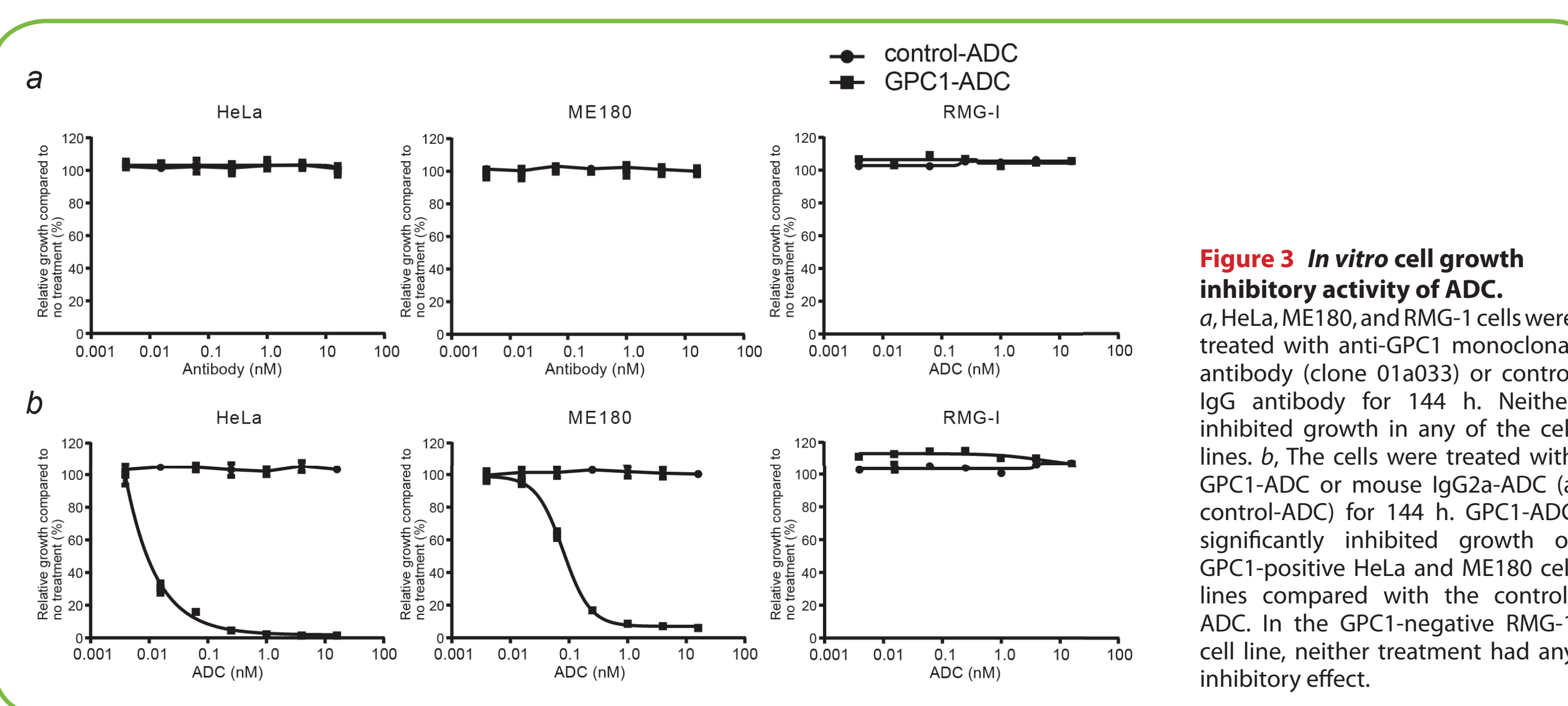


**Figure 3** *In vitro* cell growth inhibitory activity of ADC.

*a*, HeLa, ME180, and RMG-1 cells were treated with anti-GPC1 monoclonal antibody (clone 01a033) or control IgG antibody for 144 h. Neither inhibited growth in any of the cell lines. *b*, The cells were treated with GPC1-ADC or mouse IgG2a-ADC (a control-ADC) for 144 h. GPC1-ADC significantly inhibited growth of GPC1-positive HeLa and ME180 cell lines compared with the control-ADC. In the GPC1-negative RMG-1 cell line, neither treatment had any inhibitory effect.

The growth of ME180 tumors in the group treated with control-ADC was similar to that in the PBS group (Figure 4*a*). In the two groups treated with 1 mg/kg or 3 mg/kg of GPC1-ADC, tumor growth was significantly suppressed compared with that in the control-ADC group after day 8 and day 12, respectively ( $p < 0.05$ ; Figure 4*a*). Importantly, after day 8, 10 mg/kg of GPC1-ADC significantly suppressed tumor growth even further than did the lower doses as compared with control-ADC ( $p < 0.001$ ; Figure 4*a*). HeLa tumor growth was significantly less than in control-treated mice for the groups treated with 3 mg/kg ( $p < 0.01$ ; after day 20) and 10 mg/kg ( $p < 0.01$ ; after day 16) of GPC1-ADC (Figure 4*b*). There was no significant difference in tumor volume between the group using 10 mg/kg of unconjugated anti-GPC1 mAb and the control IgG group in either the ME180 or HeLa xenograft model. A marked increase in the percentage of tumor cells in mitosis was detected following treatment with GPC1-ADC but not with the control-ADC (Figure 4*c*). Administration of GPC1-ADC (3, 15, 50 mg/kg) did not result in significant weight loss compared with the group treated with control-ADC (50 mg/kg).

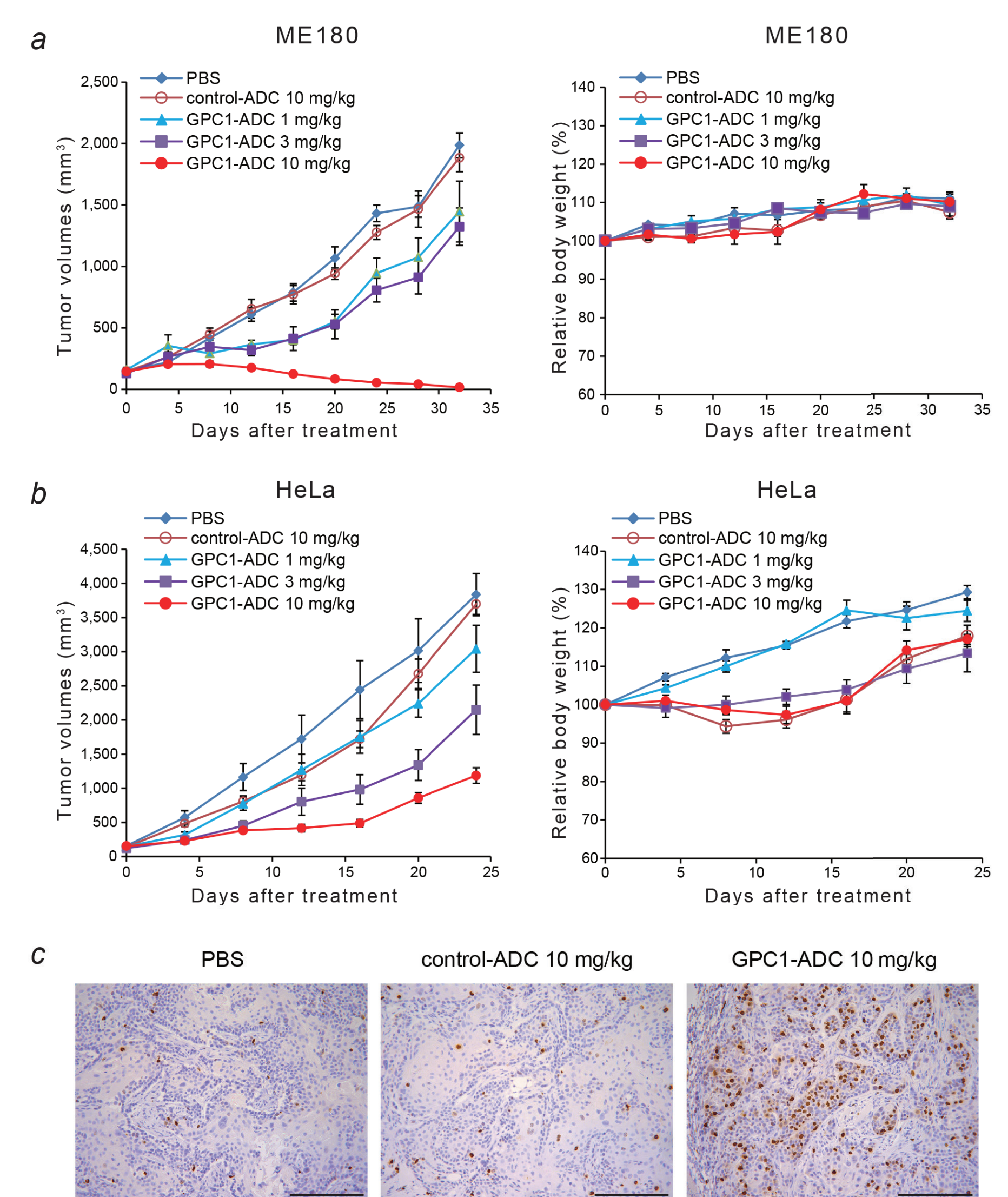


**Figure 4** Antitumor activity of GPC1-ADC *in vivo*.

*a* and *b*, Antitumor efficacy of GPC1-ADC in ME180 ( $n = 7$ /group) and HeLa ( $n = 6$ /group) xenograft models. The tumor-bearing mice were given PBS, control-ADC (10 mg/kg), or GPC1-ADC (1, 3, 10 mg/kg) intravenously on days 0, 4, 8, and 12. Each point on the graph represents the average tumor volume. Changes in body weight are also represented. *c*, GPC1-ADC causes mitotic arrest *in vivo*. Animals bearing ME180 tumor xenografts were given a single dose of PBS, control-ADC (10 mg/kg), or GPC1-ADC (10 mg/kg). After 24 h, the tumors were harvested and stained with anti-phospho-histone H3 (Ser10) antibody to detect mitotic cells.

- No severe adverse effects on hematopoietic cells.
- It was not high when the actual therapeutic dose of 15 mg/kg was administered.
- There were no abnormal results specific to GPC1-ADC.

Marked inflammatory cell infiltrates in the liver of both groups when treated with 50 mg/kg but only a mild inflammatory cell infiltrate in the GPC1-ADC group treated with 15 mg/kg. The 50 mg/kg dose was associated with increased numbers of macrophages and disorder of the follicular structure in the spleen in both the control-ADC group and the GPC1-ADC group.

## DISCUSSION

The ADC targeting GPC1 showed potent efficacy both *in vitro* and *in vivo* with limited toxicity. We found that the anti-GPC1 mAb was rapidly internalized into cells after binding to GPC1 on cancer cells, suggesting that GPC1 was a suitable target for constructing an ADC and that the anti-GPC1 mAb clone 01a033 was the most suitable clone, as it had high internalizing activity. Our *in vitro* ADC assay showed that HeLa and ME180 cancer cells highly expressing GPC1 were highly sensitive to GPC1-ADC, while RMG-1 cells with low expression of GPC1 were insensitive to GPC1-ADC. This suggests that certain expression levels of GPC1 seem to be required for GPC1-ADC to effectively inhibit cancer cells. By using GPC1-ADC, a significant antitumor effect was observed in both ME180- and HeLa-xenografted mice (Figures 4*a* and *b*). In addition, G2/M phase cell cycle arrest was specifically induced in tumor cells by the MMAF delivered by the GPC1-ADC (Figure 4). IHC analysis of xenografted tumor tissues indicated that GPC1 expression levels were homogeneous in tumor cells induced by both cell lines (data not shown). The difference of sensitivity to GPC1-ADC of these two xenograft models might therefore be attributed to differences in the tumor growth rate, as HeLa-induced tumors grew much more rapidly than did ME180-induced tumors *in vivo* (Figure 4). We thus demonstrated a significant antitumor effect in mouse models by conjugating an anti-GPC1 mAb (01a033) with MMAF. Importantly, we confirmed that GPC1 expression in uterine cervical cancer was detected not only in primary tumors but also in one that had relapsed after chemoradiation therapy.

## Acknowledgments

We would like to thank Y. Kanazawa, Y. Yamamoto, K. Sakiyama, and H. Abe for their secretarial assistance. We also thank E. Harada and R. Nishi for their technical assistance.

**Financial support:** This research was supported in part with funds from the Research on Development of New Drugs from Japan Agency for Medical Research and Development, AMED (16ak0101024h0003) to T.N. and the Japanese Ministry of Education, Science, Sports, and Culture Grant-in-Aid for Scientific Research (C) (16K07193) to S.S.